

## Organic fouling development in a long channel RO membrane cell

H. Mo and H. Y. Ng

### ABSTRACT

This study was to experimentally investigate organic fouling development in a 1-m long RO membrane channel using alginate as a model organic compound. Five parallel local permeate fluxes with a distance interval of 20 cm along the channel were monitored continuously during the organic filtration tests. It was found that organic fouling became more severe towards the outlet of the channel. This might be mainly attributed to the salt concentration polarization formation along the channel. The higher salt concentration downstream increased the interactions involved in organic fouling such as charge-screening and alginate-calcium bridging, which intensively promoted organic fouling formation in the downstream. A higher feed flow was a common option to mitigate fouling at most lab-scale RO research work, but not the case in this long membrane channel. A higher feed flow changed the organic fouling development profile along the channel, but would not eliminate organic fouling.

**Key words** | concentration polarization, long channel, organic fouling, reverse osmosis (RO)

**H. Mo** (corresponding author)  
Department of Civil Engineering,  
National University of Singapore,  
1 Engineering Drive 2, E1A-07-03,  
Singapore 117576,  
Singapore  
E-mail: g0403666@nus.edu.sg

**H. Y. Ng**  
Centre for Water Research, Division of  
Environmental Science & Engineering,  
National University of Singapore,  
Singapore 119260,  
Singapore  
E-mail: esenghy@nus.edu.sg

### INTRODUCTION

Fouling control is crucial to the success of RO membrane processes in water reuse or desalination. Various chemicals, pretreatment technologies and processes are available for fouling control. However, the choosing of these chemicals, pretreatment technologies and processes is difficult without a correct characterization of specific feed water fouling tendency and fouling prediction in a specific full-scale RO process. Compared with fouling research work conducted at lab-scale using small RO membrane cell, full-scale RO processes featured a long channel via a few membrane modules connected in series in a pressure vessel. The former was commonly treated as a homogenous system. Accordingly, based on homogenous membrane system most membrane fouling models assume uniform flow properties and fouling rate throughout the membrane surface. However, it has been reported that the long RO channel could not be treated as a homogenous system due to the variant operating parameters (e.g. crossflow velocity and salt concentration in the bulk solution) along the

channel (Song & Tay 2006). Hence, those models are unrealistic to predict the organic fouling development for full-scale RO processes.

According to our previous experimental work on one 1-m RO long channel, the hydrodynamic parameters and water chemistry in bulk solution changed along the RO channel and did not remain the same with the feed water and applied conditions (Mo & Ng 2010). The permeate flux decreased along the channel and salt concentration in the bulk solution increased exponentially along the channel. These parameters have been reported to be significant factors in organic fouling of RO membrane (Lee *et al.* 2006; Ang & Elimelech 2007). Therefore, the foulant deposition does not only evolve with time, but also distributes spatially along the feed channel. From an example of a two-stage RO train in a pilot-scale water reclamation plant, the heterogeneous development of foulant deposition along the channel was observed (Schneider *et al.* 2005). The proportion of organic matters in the fouling layer increased in

doi: 10.2166/ws.2010.180

the first stage from approximately 30% in the first two RO elements to 55% in RO elements 4–6, and remained constant for subsequent RO elements in stage 2. The spatial distribution of the fouling deposition may be ascribed to the local variation of flow, pressure, and concentration along the feed channel throughout the whole system (Schwinge *et al.* 2004; Song & Tay 2006). Therefore, the channel length is a critical factor to predict the temporal and spatial fouling development.

Two new models have been developed to describe the fouling characteristics of full-scale RO processes (Chen *et al.* 2004; Hoek *et al.* 2008). They referred a direct result of foulant deposition developing along the channel as “flux leveling”, whereby the permeate flux shifted from the inlet towards the outlet to maintain a constant global water production as fouling progressed. These two models worked impressively to predict the performance of full-scale RO processes, but some argument remained doubtful as the interactions involved in the organic fouling was not considered and no experimental data was presented to show the flux variation along the channel as well. Therefore, more experimental work in a long membrane channel was needed to provide more information for accurate assumptions and definitions in modeling work.

This study aimed to investigate organic fouling development in a 1-m long RO membrane channel using alginate as a model organic compound. During organic filtration tests, five parallel local permeate fluxes with a distance interval of 20 cm along the membrane channel was monitored continuously to monitor organic fouling development. The effect of feed flow on organic fouling was also investigated.

## MATERIALS AND METHODS

### RO testing setup and long channel RO membrane cell

The RO testing membrane setup consisted of a high pressure feeding system, five flowmeters connected to a data acquisition system and a 1-m long membrane cell (Figure 1(a)). Details of the experimental setup can be found in elsewhere (Mo & Ng 2010). Figure 1(b) shows the picture of the 1-m long RO membrane cell. This cell was

equipped with ten permeate collectors with the same distance interval from the inlet towards the end of the channel. Each two adjacent permeate collectors were connected to a flowmeter to measure the local permeate flux. A commercial RO membrane (ESPA2, Hydranautics, CA) with an effective filtration area of 300 cm<sup>2</sup> (3 × 100 cm) was used.

### Filtration experiments

After the RO membrane system was flushed with demineralized (DI) water (Milli-Q, Millipore), fresh RO membrane was first compacted with DI water for 24 h at 300 psi (2.07 × 10<sup>6</sup> Pa). Stock solutions of salt were introduced into the feed water to achieve the required ionic strength (7 mM of NaCl and 1 mM of CaCl<sub>2</sub>) and the system was continued to operate for another 2 h at the same operating conditions. Then, the pressure was adjusted to a preset value to achieve a steady permeate flux (total overall initial flux, that is the sum of the five local initial fluxes) for about 2 h. The organic stock solution was subsequently added into the feed water to initiate the fouling process. Permeate flow was continuously recorded until the test was terminated when the permeate flux reached a predetermined value. A commercial hydrophilic biopolymer–sodium alginate (Product No. A2158, Sigma-Aldrich, Saint Louis, MO) was used as the model organic compound and its concentration was maintained as 50 mg/L. All fouling experiments were conducted at temperature of 25°C with uncontrolled feed water pH of about 6.0.

## RESULTS AND DISCUSSION

### The permeate behavior in alginate fouling along the RO membrane channel

Figure 2(a) shows the local permeate flux at five different permeate points along the 1-m RO membrane channel during the alginate fouling process. The local permeate flux referred to the flux averaged on each 20-cm filtration section. For each permeate point, flux behavior was characterized by a similar profile—rapid decline initially then gradually reaching a (pseudo-)stable flux. Due to concentration

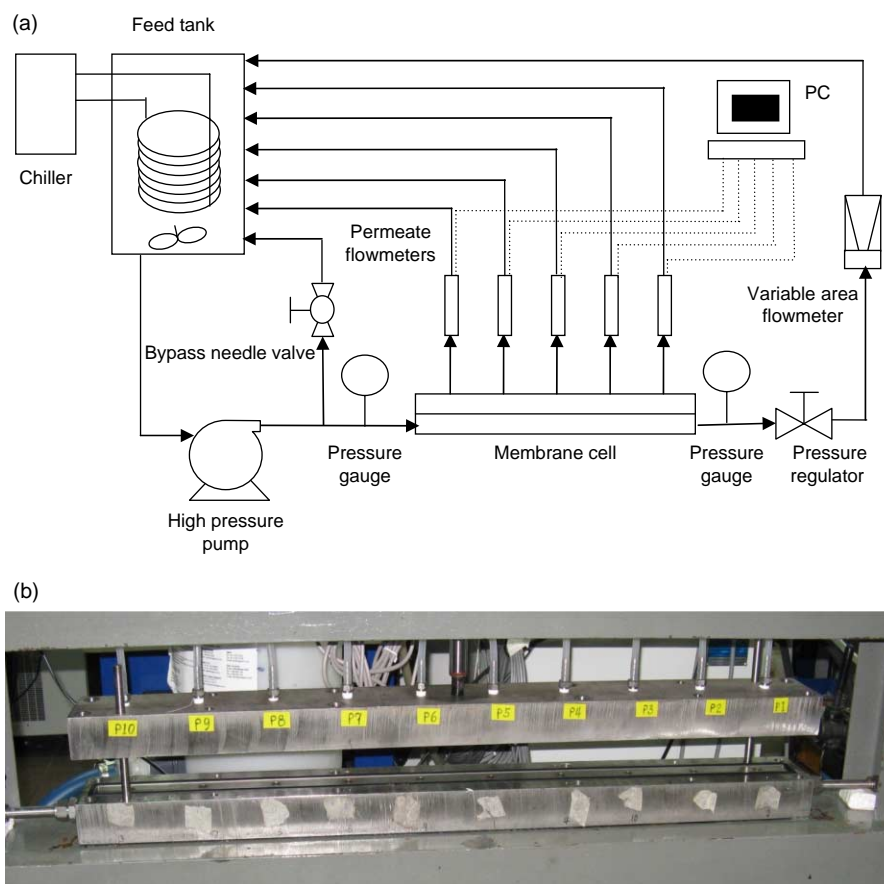


**Figure 1** | (a) Schematic diagrams of the RO setup and (b) the picture of the 1-m long RO membrane cell.

polarization of salt becoming more severe along the channel, the local initial flux decreased along the channel as shown in Figure 3. Hence, the fluxes were normalized to their corresponding local initial flux to compare the differences in fouling rate for each permeate point along the channel. Figure 2(b) shows that the normalized flux rate declined faster in the downstream compared to in the upstream, which indicates that organic fouling developed faster in the downstream than in the upstream. This observation of permeate flux being declined faster in the downstream was coincident with some reports of more foulant deposition in the latter elements in a RO train (Schneider *et al.* 2005).

Local initial flux could be a possible factor affecting the organic fouling development along the channel since the local initial flux at each permeate point was different along the channel. However, the local initial flux was lower in the downstream, thus bringing less foulants to the membrane

surface and leading to less fouling towards the end of the channel. Hence, the contribution of the local initial flux to the fouling development conflicted with the observation of alginate fouling development in this study. Therefore, one possible factor for alginate fouling becoming more severe along the channel is the concentration polarization of salt and organic foulant. On one hand, the increasing concentration of organic foulant might directly contribute to faster flux reduction along the channel but this effect was not significant (Tang & Leckie 2007). On the other hand, elevated salt concentration downstream could lead to the formation of a compact and thick fouling layer on the membrane surface due to charge-screening and alginate-calcium interactions, leaving less free alginate in the bulk stream (Grant *et al.* 1973; Lee *et al.* 2006).

One previous study has shown that more severe alginate fouling occurred at high salt concentration and in the presence of divalent cation (Lee *et al.* 2006). When salt and

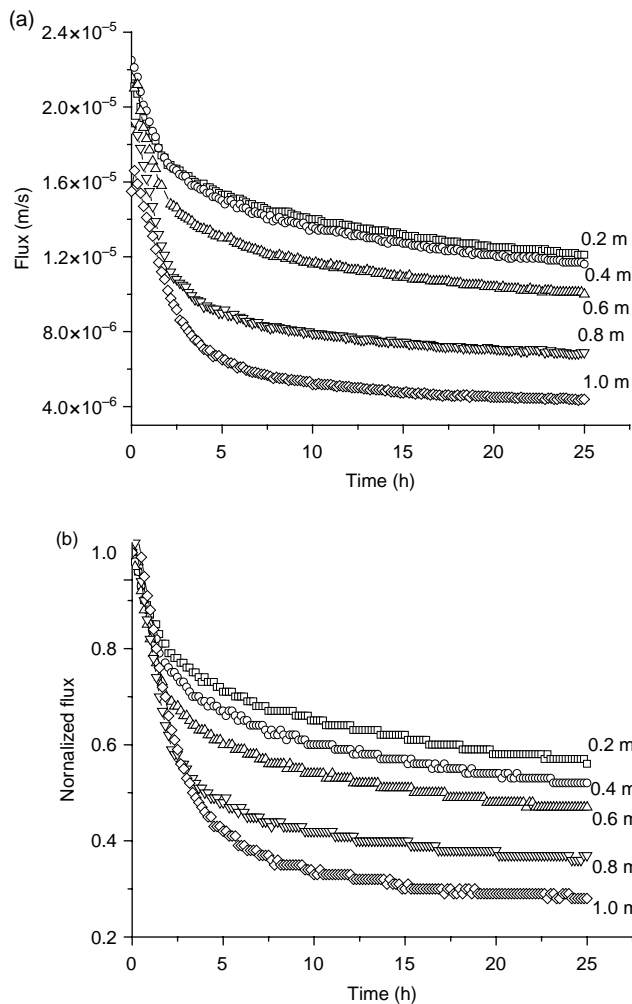


**Figure 2** | Permeate flux (a) and normalized flux (b) evolution over 25h of alginate fouling at different locations along the channel (Fouling conditions: alginate of 50 mg/L; ionic strength of 10 mM; calcium of 1.0 mM; unjust pH at  $6.0 \pm 0.1$ ; temperature of 25°C; initial flux of  $2.00 \times 10^{-5}$  m/s; feed flow velocity of 9 cm/s).

calcium concentration increased along the channel, the ratio of foulant (alginate) sticking on the membrane over the total foulant convected towards the membrane surface increased along the channel. This ratio is crucial for investigating organic fouling development quantitatively.

#### Variation of membrane resistance along the channel

A resistance-in-series model is commonly used to describe the flux behavior (Mulder 1996). In this model, foulant is deposited on the membrane surface to form a cake layer and the cake layer resistance is in series with the membrane resistance. According to the principle of membrane

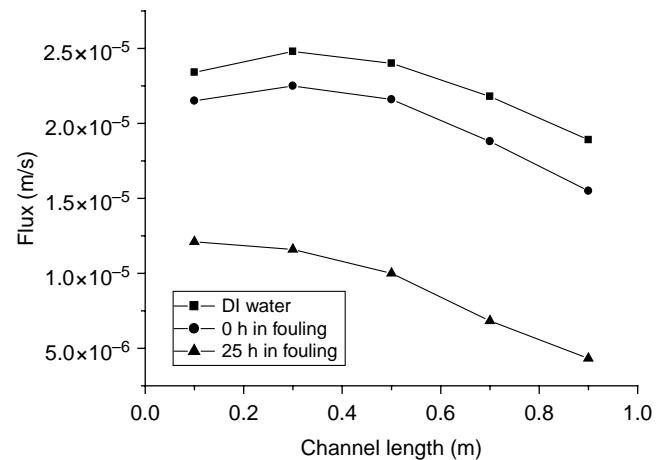


**Figure 3** | The permeate flux profile along the channel in DI water filtration and alginate fouling process (DI water filtration: unjust pH at  $6.0 \pm 0.1$ ; temperature of 25°C; feed flow velocity of 9 cm/s. Fouling conditions: alginate of 50 mg/L; ionic strength of 10 mM; calcium of 1.0 mM; unjust pH at  $6.0 \pm 0.1$ ; temperature of 25°C; total initial flux of  $2.00 \times 10^{-5}$  m/s; feed flow velocity of 9 cm/s).

transfer and resistance-in-series, the permeate flux is given by Equation (1)

$$v_p = \frac{\Delta p - \Delta \pi}{R_m + R_f} \quad (1)$$

where  $v_p$ ,  $\Delta p$ ,  $\Delta \pi$ ,  $R_m$  and  $R_f$  are the permeate flux, transmembrane pressure, osmotic pressure, membrane resistance and fouling layer resistance, respectively. Three factors—membrane, concentration polarization layer and fouling layer contribute to reduction of permeate flux. The contribution of concentration polarization layer could be defined as a “resistance” to permeate flux,  $R_\pi$ , as an equivalence of osmotic pressure (Denisov 1994). Hence,  $v_p$  could be expressed in another way as Equation (2).

$$v_p = \frac{\Delta p}{R_m + R_\pi + R_f} \quad (2)$$

In this study of using a 1-m long RO membrane channel, the determination of local permeate flux took into consideration of time and location and was expressed in Equation (3)

$$v_p(x, t) = \frac{\Delta p(x, t)}{R_0(x, t) + R_\pi(x, t) + R_f(x, t)} \quad (3)$$

where  $t$  is time of filtration and  $x$  is the distance from the inlet of RO membrane channel. The transmembrane

pressure  $\Delta p(x,t)$  was assumed to be constant along the channel during the whole fouling process because the pressure sensors did not detect significant pressure variation in this 1-m membrane cell. Hence, the applied pressure  $\Delta p$  was used to replace  $\Delta p(x,t)$ . Osmotic pressure  $\Delta \pi(x,t)$  was assumed to be caused mainly by salt and not to be affected by organics in this study since its concentration was negligible compared to the salt concentration in the feed, although we recognized that this might be a simplification since the concentration of macromolecules might have appreciable osmotic pressure in the same order of magnitude as applied pressure generally used in UF (Clifton *et al.* 1984; Sablani *et al.* 2001). Additionally, the osmotic pressure was assumed not to be affected by the fouling layer formation (Lee *et al.* 2005). Hence,  $\Delta \pi(x,t)$  was the function of only channel length,  $\Delta \pi(x)$ , and thus the equivalent resistance of concentration polarization layer also depended on channel length. Therefore, the expression of the permeate flux was modified to be more applicable to this long channel as the following Equation (4)

$$v_p(x,t) = \frac{\Delta p}{R_t(x,t)} = \frac{\Delta p}{R_m(x) + R_\pi(x) + R_f(x,t)} \quad (4)$$

where  $R_t$  is the total resistance.

The three types of resistance could be calculated from three permeate fluxes at different time. Membrane resistance could be determined from the DI water flux,  $v_m(x)$ , just after 25 h of DI water compaction when no concentration polarization and fouling occurred (Mo & Ng 2010) (Equation (5)).

$$R_m(x) = \frac{\Delta p}{v_m(x)} \quad (5)$$

The second flux,  $v_\pi(x)$ , was the initial flux at the beginning of the fouling process, which was determined just before foulant introduction into the feed solution when concentration polarization was formed and the fouling layer resistance was zero.  $R_\pi$  was determined from Equation (6).

$$R_\pi(x) = \frac{\Delta p}{v_\pi(x)} - R_m(x) \quad (6)$$

The third flux,  $v_p(x,t)$ , was the final flux at the end of the 25-h fouling process. The fouling resistance was calculated

according to Equation (7).

$$R_f(x,t) = \frac{\Delta p}{v_p(x,t)} - R_m(x) - R_\pi(x) \quad (7)$$

Figure 3 shows the three permeate flux profiles along the channel—DI water flux before fouling formation, initial flux and final flux in the fouling process. The DI water flux was resisted by the membrane itself. It was noted that the DI water flux was not uniform along the channel, which could be explained by the membrane resistance as shown in Figure 4. The membrane resistance was higher in the two ends than in the middle of the RO membrane. The introduction of salt into the feed water resulted in lower permeate fluxes due to concentration polarization. A typical characteristic was that the flux decline from the corresponding DI water flux became larger from the inlet to the outlet, that is, the flux was reduced by 18.3% for the first permeate location while 36.4% for the fifth permeate location. This indicated that the salt concentration build-up in the boundary layer on the membrane surface was not even along the channel. Correspondingly, the equivalent resistance of concentration polarization layer was larger towards the outlet of the RO membrane channel as shown in Figure 4. The equivalent resistance of concentration polarization layer had a small fraction of the total resistance compared to the fouling layer resistance which contributed to more than 50% of the total resistance. The fouling layer resistance profiles along the channel had an exponential

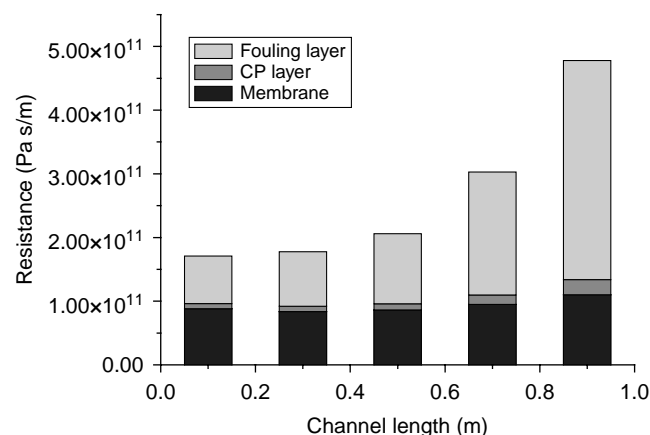


**Figure 4** | Three types of resistance along the RO membrane channel (Fouling conditions: alginate of 50 mg/L; ionic strength of 10 mM; calcium of 1.0 mM; unadjusted pH at  $6.0 \pm 0.1$ ; temperature of 25°C; total initial flux of  $2.00 \times 10^{-5}$  m/s; feed flow velocity of 9 cm/s).

growth, which demonstrated the uneven development of organic fouling along the membrane channel.

### Effects of feed flow on alginate fouling development along the channel

Operating conditions are of interest because they are easily adjusted to create different hydrodynamic conditions to study organic fouling in macro-level and to control fouling in practice as well. Hence, organic fouling tests were conducted to investigate alginate fouling development along the RO membrane for different feed flow velocities.

The effects of feed flow velocity on the alginate fouling development along the 1-m long RO membrane channel was shown in Figure 5, which plots the fouling extent in terms of the normalized flux at each permeate point after 25 h of organic fouling under different feed flow velocities or inlet feed flow velocities (3, 9, 23, and 36 cm/s). It was noted that the effect of feed flow velocity on organic fouling was complicated by the channel effect. In the upstream of the channel, lower feed flow velocity resulted in more severe fouling extent due to lower shear rate sweeping less foulant away from the membrane surface, which is consistent with most RO studies using small lab-scale RO setup in which the membrane channel effect was negligible. After the middle point of the channel, the fouling trend reversed, that is, a higher feed flow velocity contributed to more

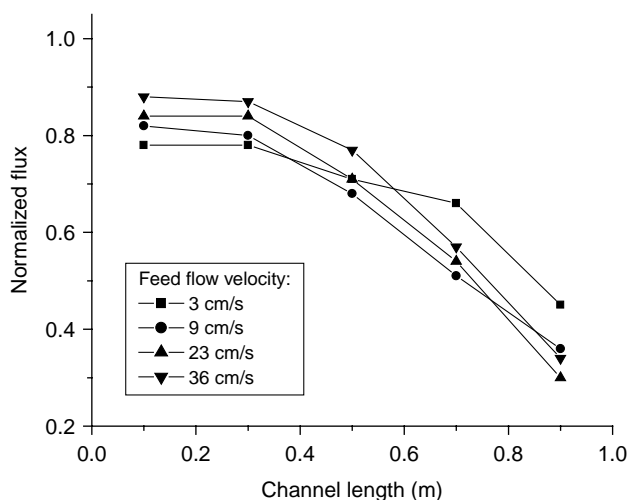


**Figure 5** | Effects of feed flow velocity on alginate fouling along the channel (Fouling conditions: alginate of 50 mg/L; ionic strength of 10 mM; calcium of 1.0 mM; unjust pH at  $6.0 \pm 0.1$ ; temperature of 25°C; total initial flux of  $1.32 \times 10^{-5}$  m/s).

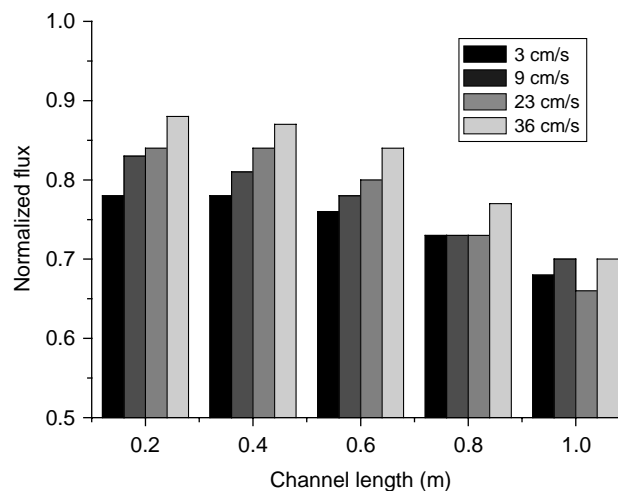


**Figure 6** | Accumulative normalized flux after 25-h organic fouling over different length of the RO membrane channel (Fouling conditions: alginate of 50 mg/L; ionic strength of 10 mM; calcium of 1.0 mM; unjust pH at  $6.0 \pm 0.1$ ; temperature of 25°C; total initial flux of  $1.32 \times 10^{-5}$  m/s).

severe fouling. This is possibly due to the fact that a higher feed flow velocity swept more foulant into the bulk solution in the upstream of the membrane channel, which favorably enabled the downstream permeate flux to bring more foulant towards the membrane surface.

Therefore, the effect of feed flow velocity was to change the foulant distribution along the membrane channel instead of mitigating fouling in the membrane channel. Figure 6 shows the accumulative normalized flux over the different length of membrane channel. It was found that when the channel was up to 1 m, the flux reduction was similar for four cases of feed flow. This implied significant interactions between membrane setup design and operating conditions. For example of feed flow of 23 cm/s, a channel of 0.8 m is the best channel length to control fouling. If the longer channel than 0.8 m was designed, more flux reduction occurred in the feed flow of 23 cm/s than the feed flow of 3 cm/s.

## CONCLUSIONS

The research work in this study experimentally investigated local permeate flux decline in the fouling development of hydrophilic biopolymer–sodium alginate along a 1-m RO membrane channel. Local permeate flux behavior showed that organic fouling development was a heterogeneous

process in a long membrane channel. The fouling of RO membrane by alginate was faster and more severe in the downstream than in the upstream of the membrane channel. In addition, three types of local resistance along the channel were calculated and compared. Except the membrane resistance which was considered to be constant after 24 h of compaction and over the relatively short duration of fouling test (25 h), the resistance of the concentration polarization layer and fouling layer increased from the inlet to outlet of the membrane channel. Fouling layer contributed to a significant fraction of the total resistance and hence the permeate reduction.

The uneven development of alginate fouling along the RO membrane channel might be attributed to the concentration polarization formation and other hydrodynamic condition variation along the long membrane channel. Higher downstream salt concentration at the membrane surface enhanced the interactions between the salt and alginate, such as charge-screening and calcium-alginate bridging. As a result, a higher fraction of alginate adhered to the membrane surface. In addition, high feed flow velocity swept more organic foulant away from the membrane surface in the upstream, but accordingly shifted more organics towards the downstream, which contributed to more severe organic fouling formation in the downstream.

## REFERENCES

- Ang, W. S. & Elimelech, M. 2007 Protein (BSA) fouling of reverse osmosis membranes: implications for wastewater reclamation. *J. Membr. Sci.* **296**, 83–92.
- Chen, K. L., Song, L. & Ng, W. J. 2004 The development of membrane fouling in full-scale RO processes. *J. Membr. Sci.* **232**, 63–74.
- Clifton, M. J., Abidine, N., Aptel, P. & Sanchez, V. 1984 Growth of the polarization layer in ultrafiltration with hollow-fiber membranes. *J. Membr. Sci.* **21**, 233–246.
- Denisov, G. A. 1994 Theory of concentration polarization in cross-flow ultrafiltration gel-layer model and osmotic-pressure model. *J. Membr. Sci.* **91**, 173–187.
- Grant, G. T., Morris, E. R., Rees, R. A., Smith, P. J. C. & Thom, D. 1973 Biological interactions between polysaccharides and divalent cations: the egg-box model. *FEBS Lett.* **32**, 195–198.
- Hoek, E. M. V., Allred, J., Knoell, T. & Jeong, B.-H. 2008 Modeling the effects of fouling on full-scale reverse osmosis processes. *J. Membr. Sci.* **314**, 33–49.
- Lee, S., Cho, J. & Elimelech, M. 2005 Combined influence of natural organic matter (NOM) and colloidal particles on nanofiltration membrane fouling. *J. Membr. Sci.* **262**, 27–41.
- Lee, S., Ang, W. S. & Elimelech, M. 2006 Fouling of reverse osmosis membranes by hydrophilic organic matter: implications for wastewater reuse. *Desalination* **187**, 313–321.
- Mo, H. & Ng, H. Y. 2010 An experimental study on the effect of spacer on concentration polarization in a long channel reverse osmosis membrane cell. *Water Sci. Technol.* **61**(8), 2035–2041.
- Sablani, S. S., Goosen, M. F. A., Al-Relushi, R. & Wilf, M. 2001 Concentration polarization in ultrafiltration and reverse osmosis: a critical review. *Desalination* **141**, 269–289.
- Schneider, R. P., Ferreira, L. M., Binder, P. & Ramos, J. R. 2005 Analysis of foulant layer in all elements of an RO train. *J. Membr. Sci.* **261**, 152–162.
- Schwinge, J., Neal, P. R., Wiley, D. E., Fletcher, D. F. & Fane, A. G. 2004 Spiral wound modules and spacers review and analysis. *J. Membr. Sci.* **242**, 129–153.
- Song, L. & Tay, K. G. 2006 Performance prediction of a long crossflow reverse osmosis membrane channel. *J. Membr. Sci.* **281**, 163–169.
- Tang, C. Y. & Leckie, J. O. 2007 Membrane independent limiting flux for RO and NF membranes fouled by humic acid. *Environ. Sci. Technol.* **41**, 4767–4773.